



Elastic properties and electronic structures of 4d- and 5d-transition metal mononitrides

W. Chen, J.Z. Jiang*

International Center for New-Structured Materials (ICNSM), Zhejiang University and Laboratory of New-Structured Materials, Department of Materials Science and Engineering, Zhejiang University, Zheda Road 38, Hangzhou 310027, PR China

ARTICLE INFO

Article history:

Received 3 February 2010

Received in revised form 18 March 2010

Accepted 18 March 2010

Available online 25 March 2010

Keywords:

Transition metal alloys and compounds

Elasticity

Electronic properties

Phase transitions

ABSTRACT

Elastic properties and electronic structures of 4d-transition metal mononitrides (ZrN, NbN, MoN, TcN, RuN, RhN, PdN, and AgN) and 5d-transition metal mononitrides (HfN, TaN, WN, ReN, OsN, IrN, PtN, and AuN) with both rocksalt and zinc-blende structures have been investigated by first-principles calculations. Lattice constants, bulk moduli, band structures and cohesive energies are obtained. The trends of lattice constants, cohesive energies and electronic properties as a function of the number of d electrons are revealed. The relationships of cohesive energies as a function of unit-cell volume and the transition pressures of zinc-blende-to-rocksalt phase transformations are also discussed.

© 2010 Elsevier B.V. All rights reserved.

1. Introduction

Metal nitrides have attracted increasing attention from both experimental and theoretical points of view because of their excellent properties such as hardness, superconductivity, photoluminescence and various types of magnetism [1–8]. Most of these studies focus on nitrides of early-transition metals or late-transition metals in 3d series. Reports on binary noble metal nitrides (i.e. Ru, Rh, Pd, Ag, Os, Ir, Pt, and Au) are very rare. Recently, Pt, Ir, Os and Pd nitrides have been synthesized under extreme conditions [9–12], which has triggered considerable interests to investigate the crystalline structures, elastic stabilities and electronic structures of novel noble metal nitrides [13–29]. Gregoryanz et al. [9] first reported that platinum nitride has a composition close to PtN with a zinc-blende structure, which was supported by three theoretical works [13–15]. Contrary to these studies, other studies proposed that the reported platinum nitride might be PtN₂ with fluorite structure [16,17] or pyrite structure [10,18]. Until now, the crystal structures of platinum nitride, iridium nitride, osmium nitride and palladium nitride are accepted to be pyrite structure, CoSb₂ structure, marcasite structure and pyrite structure, respectively [19–29]. These results are amazing because early-transition metal nitrides almost have rocksalt structure, while in the case of some late-transition metal nitrides, their structures are zinc-blende structure [30]. Some studies about 4d- and 5d-transition metal

mononitrides have also been carried out [31–34]. In this work, we present results of elastic stabilities and electronic structures for 4d-transition metal mononitrides (ZrN, NbN, MoN, TcN, RuN, RhN, PdN, and AgN) and 5d-transition metal mononitrides (HfN, TaN, WN, ReN, OsN, IrN, PtN, and AuN) with both rocksalt and zinc-blende structures by first-principles calculations. The trends of lattice constants, cohesive energies and electronic properties as a function of the number of d electrons are revealed. The relationships of cohesive energies as a function of unit-cell volume and the transition pressures of zinc-blende-to-rocksalt phase transformations are also investigated.

2. Theoretical scheme

The calculations were performed using CASTEP code [35] based on density functional theory. The interactions between the ions and the electrons are described by using the Vanderbilt ultrasoft pseudopotential [36]. Both the local density approximation (LDA) [37] and generalized gradient approximation (GGA) parameterized by Perdew, Burke, and Ernzerhof (PBE) [38] were used for the exchange-correlation potentials. The calculations were performed using an energy cutoff of 500 eV for the plane wave basis set. Integrations in the Brillouin zone were performed using *k* points generated with 10 × 10 × 10 mesh grids for both rocksalt and zinc-blende structures. The changes of the total energies with the number of *k* points and the cutoff energy were tested to ensure the convergence (<10⁻³ eV). The calculated total energy versus unit-cell volume was fitted with the Murnaghan equation of state [39].

* Corresponding author. Tel.: +86 57187952107; fax: +86 57187952107.

E-mail address: jiangjz@zju.edu.cn (J.Z. Jiang).

Table 1

The calculated lattice parameters (a in Å) and elastic constants C_{ij} , bulk modulus B , shear modulus G , Young's modulus E , and Poisson's ratio ν of mononitrides with rocksalt structure. All elastic constants except ν are in GPa. S: stable and US: unstable.

		a	C_{11}	C_{12}	C_{44}	B	G	E	ν	Stability
ZrN	GGA	4.57	462	141	143	248	152	396	0.23	S
	LDA	4.52	547	150	147	282	193	483	0.21	S
	Exp.	4.54 ^a	471 ^b	88 ^b	138 ^b	215 ^b , 248 ^c	160 ^b	443 ^b	0.16 ^b	
NbN	GGA	4.41	692	113	84	306	187	660	0.14	S
	LDA	4.36	806	119	89	348	216	776	0.13	S
	Exp.	4.39 ^a	608 ^b	134 ^b	117 ^b	292 ^b , 348 ^c	165 ^b	560 ^b	0.18 ^b	
MoN	GGA	4.33	305	344	-25	331	-22	-59	0.53	US
	LDA	4.27	347	389	-21	375	-21	-64	0.53	US
TcN	GGA	4.29	575	211	-162	333	10	461	0.27	US
	LDA	4.23	678	230	-193	379	16	562	0.25	US
RuN	GGA	4.29	317	299	-155	305	-73	27	0.49	US
	LDA	4.22	421	330	-191	361	-73	130	0.44	US
RhN	GGA	4.35	462	198	56	286	94	344	0.30	S
	LDA	4.30	498	251	13	333	68	331	0.33	S
PdN	GGA	4.40	345	178	50	234	67	224	0.34	S
	LDA	4.33	435	213	46	287	79	294	0.33	S
AgN	GGA	4.59	231	120	30	157	43	148	0.34	S
	LDA	4.50	292	153	22	200	46	186	0.34	S
HfN	GGA	4.56	561	147	100	285	154	500	0.21	S
	LDA	4.49	659	141	102	314	181	609	0.18	S
	Exp.	4.52 ^a	679 ^b	119 ^b	150 ^b	306 ^b , 260 ^c	202 ^b	644 ^b	0.15 ^b	
TaN	GGA	4.40	848	133	62	372	210	812	0.14	S
	LDA	4.39	906	140	64	395	224	868	0.13	S
	Exp.	4.39 ^a								
WN	GGA	4.46	181	358	-56	299	-72	-295	0.66	US
	LDA	4.43	216	395	-48	335	-69	-296	0.65	US
ReN	GGA	4.31	545	274	-518	364	-191	361	0.33	US
	LDA	4.26	622	296	-534	405	-185	431	0.32	US
OsN	GGA	4.33	340	328	-254	331	-124	18	0.49	US
	LDA	4.28	430	358	-296	382	-130	104	0.45	US
IrN	GGA	4.41	420	266	9	317	43	214	0.39	S
	LDA	4.36	427	331	-59	363	-6	138	0.44	US
PtN	GGA	4.50	285	223	45	243	38	90	0.44	S
	LDA	4.44	361	252	37	288	46	154	0.41	S
AuN	GGA	4.68	260	141	30	180	20	161	0.35	S
	LDA	460	341	160	26	220	58	238	0.32	S

^a Ref. [42].

^b Ref. [43].

^c Ref. [43], $k'_0 = 4.0$

In order to calculate elastic constants of a structure, a small strain is applied onto the structure then the change in energy or stress can be calculated in the structure. If the primitive cell volume of crystal has a small strain ε , the total energy $E(V, \varepsilon)$ can be expanded as a Taylor series [40],

$$E(V, \varepsilon) = E(V_0, \varepsilon) + V_0 \sum_{i=1}^6 \sigma_i \varepsilon_i + \frac{V_0}{2} \sum_{i=1}^6 c_{ij} e_i e_j + \dots \quad (1)$$

where $E(V_0, \varepsilon)$ is the energy of the unstrained system with the equilibrium volume V_0 , ε is strain tensor which is defined as [40]

$$\varepsilon = \begin{pmatrix} e_1 & \frac{1}{2}e_6 & \frac{1}{2}e_5 \\ \frac{1}{2}e_6 & e_2 & \frac{1}{2}e_4 \\ \frac{1}{2}e_5 & \frac{1}{2}e_4 & e_3 \end{pmatrix} \quad (2)$$

and C_{ij} are the elastic constants, which are response to an applied stress. Both stress and strain have three tensile and three shear components. The elastic constants form a 6×6 symmetric matrix.

We note that, there are three independent elastic constants (C_{11} , C_{12} and C_{44}) for cubic structures. In the CASTEP calculations, the distorted structures are automatically generated and compared with the ideal (initial) structure to calculate strain and stress. Bulk modulus B and shear modulus G are given as a function of elastic constants [41],

$$B = \frac{C_{11} + 2C_{12}}{3} \quad (3-a)$$

$$G = \frac{5(C_{11} - C_{12})C_{44}}{4C_{44} + 3(C_{11} - C_{12})} \quad (3-b)$$

Young's modulus E and Poisson's ratio ν are obtained by the following formulas:

$$E = \frac{9BG}{3B + G} \quad (3-c)$$

$$\nu = \frac{3B - 2G}{2(3B + G)} \quad (3-d)$$

Table 2

The calculated lattice parameters (a in Å) and elastic constants C_{ij} , bulk modulus B , shear modulus G , Young's modulus E , and Poisson's ratio ν of mononitrides with zinc-blende structure. All elastic constants except ν are in GPa. S: stable and US: unstable.

		a	C_{11}	C_{12}	C_{44}	B	G	E	ν	Stability
ZrN	GGA	4.95	250	144	60	180	57	144	0.37	S
	LDA	4.89	273	166	84	201	69	148	0.38	S
NbN	GGA	4.75	293	201	-15	231	16	129	0.41	US
	LDA	4.70	313	223	-1	253	22	127	0.42	US
MoN	GGA	4.64	244	260	-743	255	-376	-24	0.52	US
	LDA	4.58	273	292	-576	286	-293	-27	0.52	US
TcN	GGA	4.56	301	256	-51	271	-14	66	0.46	US
	LDA	4.50	323	299	-162	307	-75	36	0.48	US
RuN	GGA	4.53	289	252	104	265	61	55	0.47	S
	LDA	4.47	320	298	104	305	58	33	0.48	S
RhN	GGA	4.63	251	226	39	234	26	37	0.47	S
	LDA	4.58	287	258	44	267	29	43	0.47	S
PdN	GGA	4.71	163	190	-3	181	-8	-41	0.54	US
	LDA	4.64	201	242	-16	228	-18	-63	0.55	US
AgN	GGA	4.92	123	113	29	116	17	16	0.48	S
	LDA	4.82	156	146	34	150	20	15	0.48	S
HfN	GGA	5.02	282	160	70	201	66	165	0.36	S
	LDA	4.97	318	200	68	240	64	164	0.39	S
TaN	GGA	4.74	339	252	-21	281	11	124	0.43	S
	LDA	4.73	340	262	-26	288	7	112	0.44	S
WN	GGA	4.73	244	268	-1152	260	-582	-36	0.52	US
	LDA	4.71	290	281	-449	284	-222	13	0.49	US
ReN	GGA	4.57	215	345	-919	302	-492	-210	0.62	US
	LDA	4.54	263	364	-591	331	-321	-160	0.58	US
OsN	GGA	4.57	301	295	101	297	52	8	0.50	S
	LDA	4.52	272	367	87	337	20	-141	0.57	US
IrN	GGA	4.64	322	256	34	278	34	96	0.44	S
	LDA	4.60	354	293	38	313	34	88	0.45	S
PtN	GGA	4.79	182	219	-11	207	-15	-56	0.55	US
	LDA	4.73	205	259	-31	241	-4	-85	0.56	US
AuN	GGA	4.99	127	132	21	130	9	-7	0.51	US
	LDA	4.91	160	164	22	163	10	-6	0.51	US

3. Results and discussion

Equilibrium lattice parameters and elastic constants are listed in [Tables 1](#) and [2](#) for rocksalt structure and zinc-blende structure, respectively. The shear modulus G is deduced by $G = (C_{11} - C_{12} + 2C_{44})/4$. The elastic stability criteria for cubic crystal [\[44\]](#) at ambient conditions are $C_{44} > 0$, $C_{11} > |C_{12}|$, and $C_{11} + C_{12} > 0$. Compared to the available experimental data, LDA underestimates the lattice constants for about 1.0–1.5%, GGA goes in the opposite way. Our calculated bulk moduli fit well with the experimental results. It is found that only ZrN, NbN, RhN, PdN, AgN, HfN, TaN, PtN, and AuN are mechanically stable in rocksalt structure while only ZrN, RuN, RhN, AgN, HfN, TaN and IrN are mechanically stable in zinc-blende structure. Among the stable nitrides, only rocksalt-structured ZrN, NbN, HfN, and TaN compounds are indeed experimentally synthesized. TaN has the highest bulk modulus (372 GPa for GGA and 395 GPa for LDA) in these stable rocksalt phases while IrN has the highest bulk modulus (278 GPa for GGA and 313 GPa for LDA) in these stable zinc-blende phases. PtN, IrN and OsN either contradict elastic stability restrictions or have lower bulk moduli compared to the experimental data [\[9,11\]](#) ($B = 354$ GPa for PtN_2 , $B = 428$ GPa for IrN_2 and $B = 358$ GPa for OsN_2). Hence, the results obtained here confirm that the latest synthesized noble metal (Pt, Ir and Os) nitrides should be neither rocksalt structure nor zinc-blende structure.

The calculated band structures, at the equilibrium lattice constants, are depicted in [Figs. 1](#) and [2](#). It can be seen that all the materials are metallic in nature. For zinc-blende structure, all nitrides have the separated bands while for rocksalt structure, at Γ point, several eigenvalues occur close to each other. Harrison and Straub [\[45\]](#) describe that ZrN, NbN (4d), and HfN, TaN (5d), in the rocksalt structure, have nine and ten valence electrons per atom pair, respectively. The excess electrons occupying nonbonding bands make the compound metallic, but not significantly modify the bonding properties. Only for late-transition metal nitrides, anti-bonding states become occupied. Thus, these compounds are not stable with the rocksalt structure. Partial densities of states (PDOS) with rocksalt and zinc-blende structures are shown in [Figs. 3](#) and [4](#). Similar DOS features are found for rocksalt and zinc-blende structures. Along the series, the d-character of the valence band increases steadily with the increasing of the atomic number. The states between -18 and -12 eV are dominated by N (2s) states with a small contribution from metal atoms (M). The states above -9 eV are mainly composed of M (5d) states and N (2p) orbitals. These results indicate that a strong hybridization between the N-p states and the M-d states occurs. The central part of the DOS is characterized by two regions of high DOS separated by a low-density region. The lower region arises from the hybridization of p and d states, and the upper region is dominated by d states.

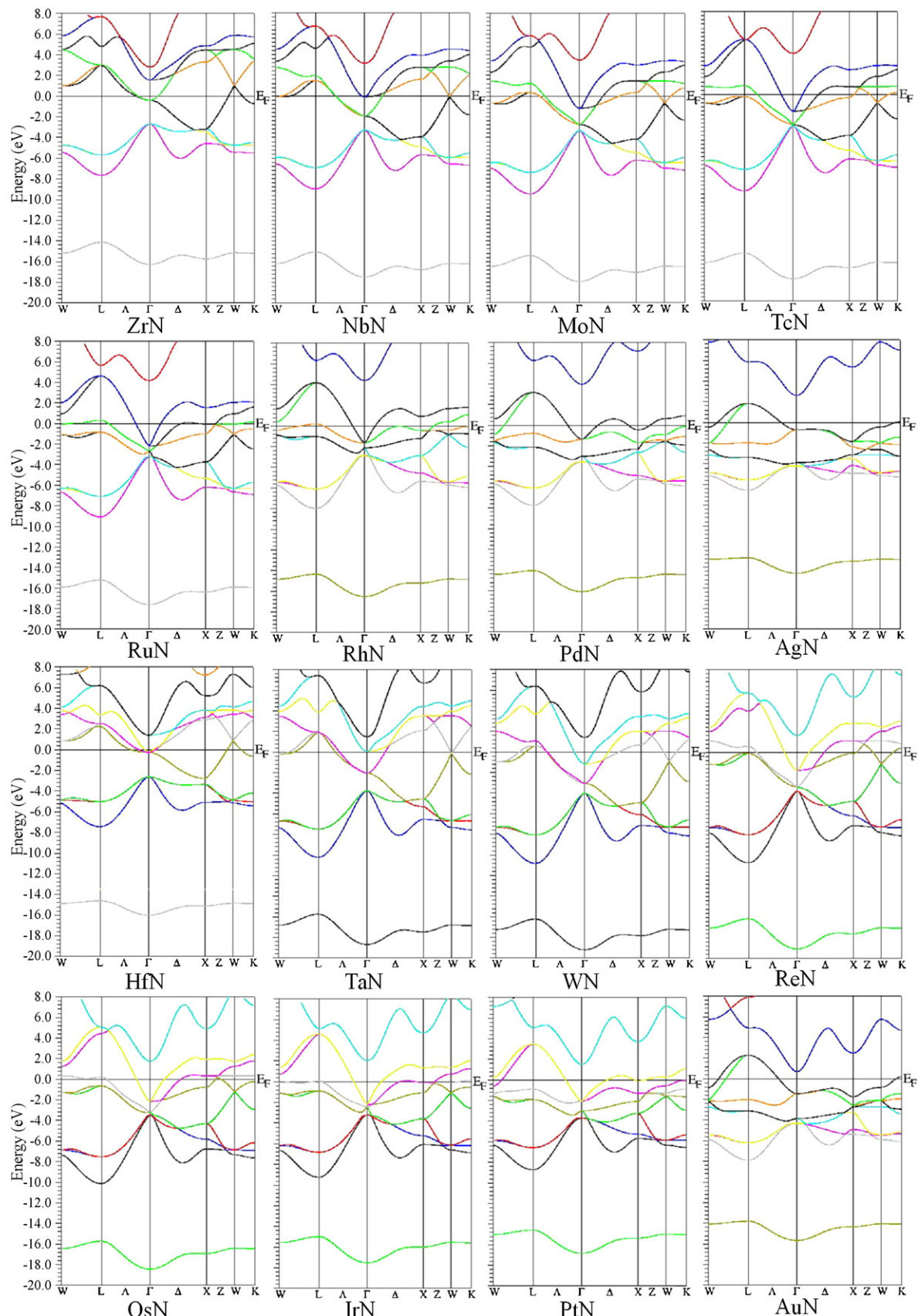


Fig. 1. Band structures of transition metal mononitrides for rocksalt structure.

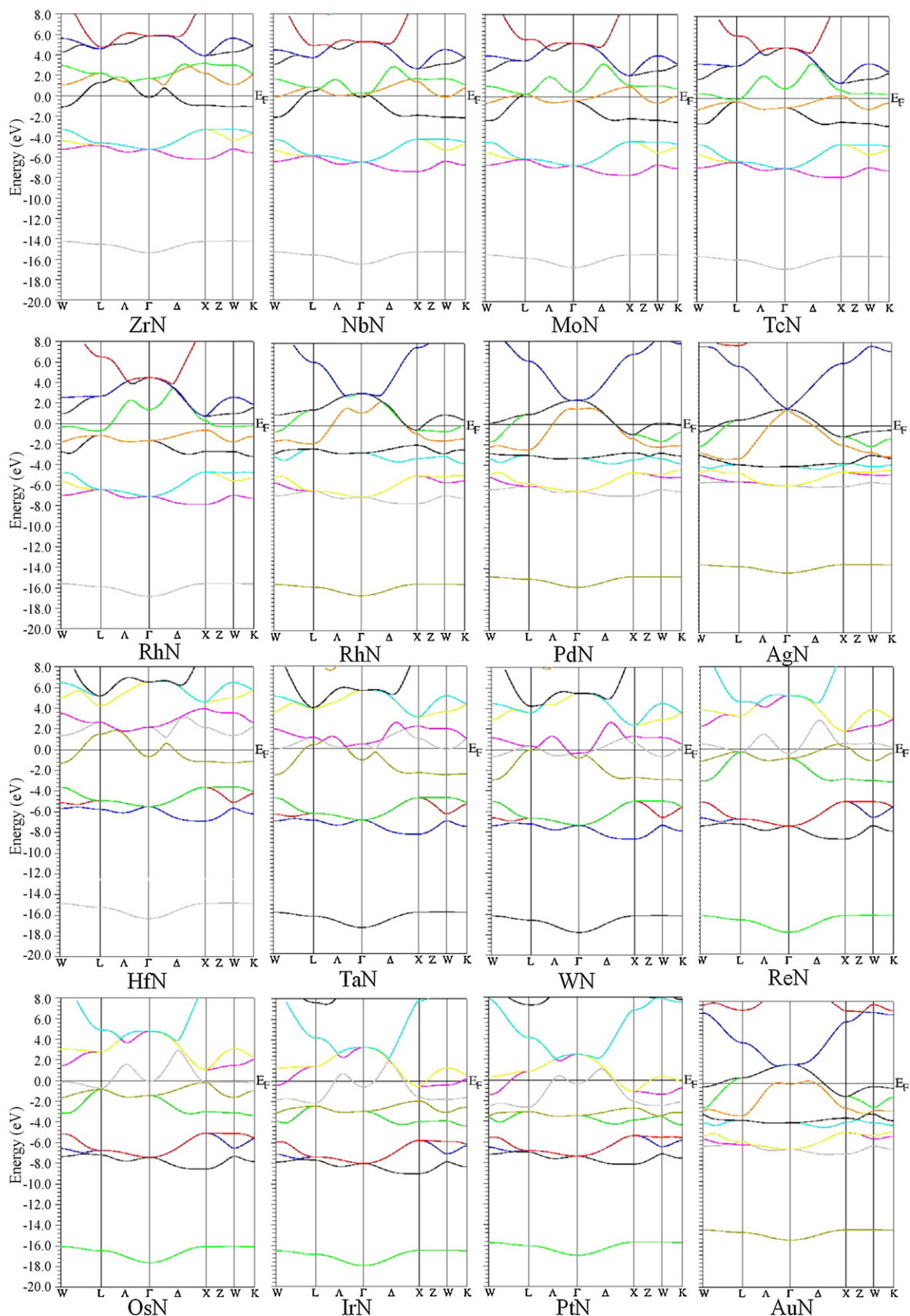


Fig. 2. Band structures of transition metal mononitrides for zinc-blende structure.

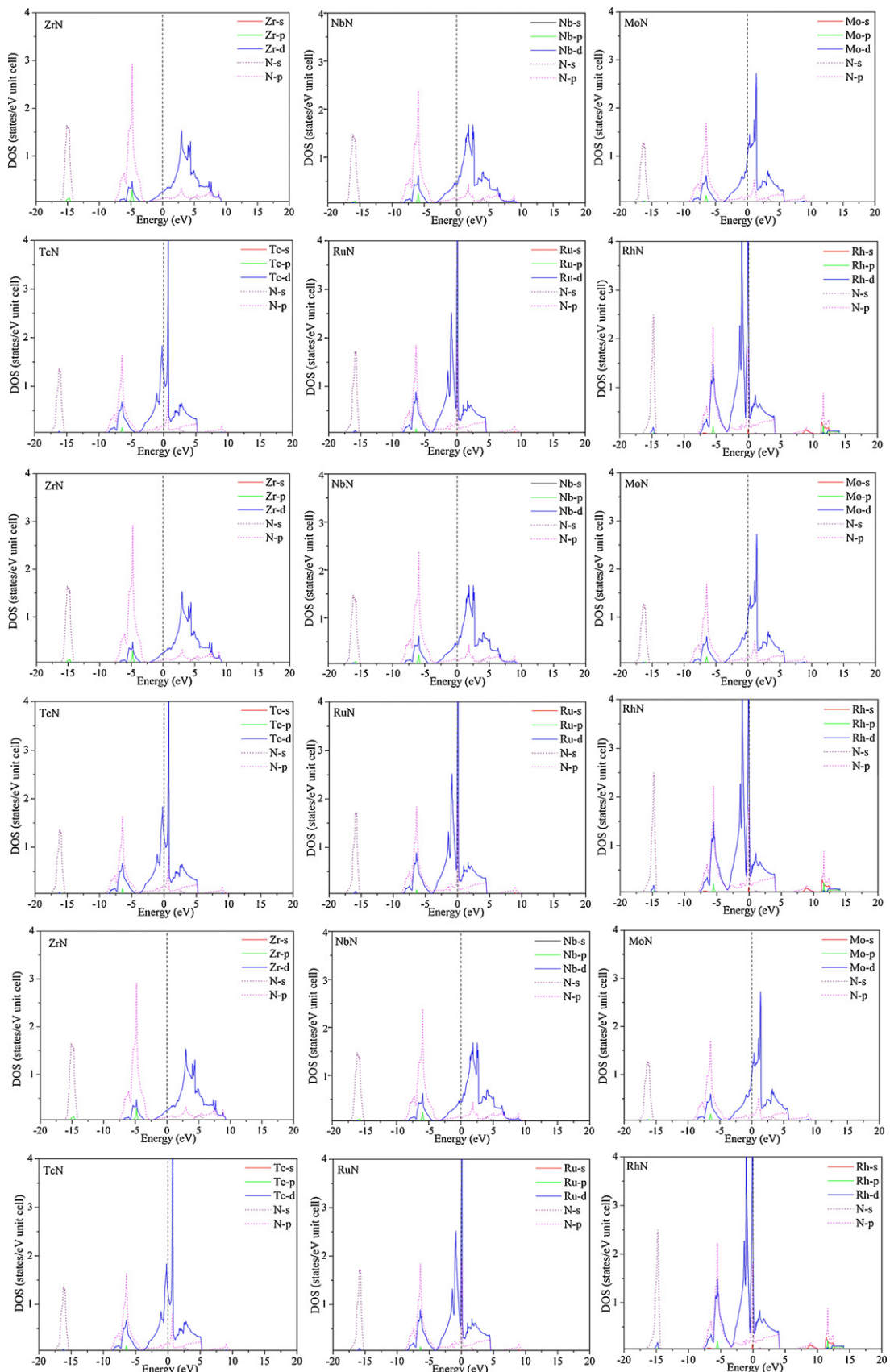


Fig. 3. Partial density of states of transition metal mononitrides for rocksalt structure.

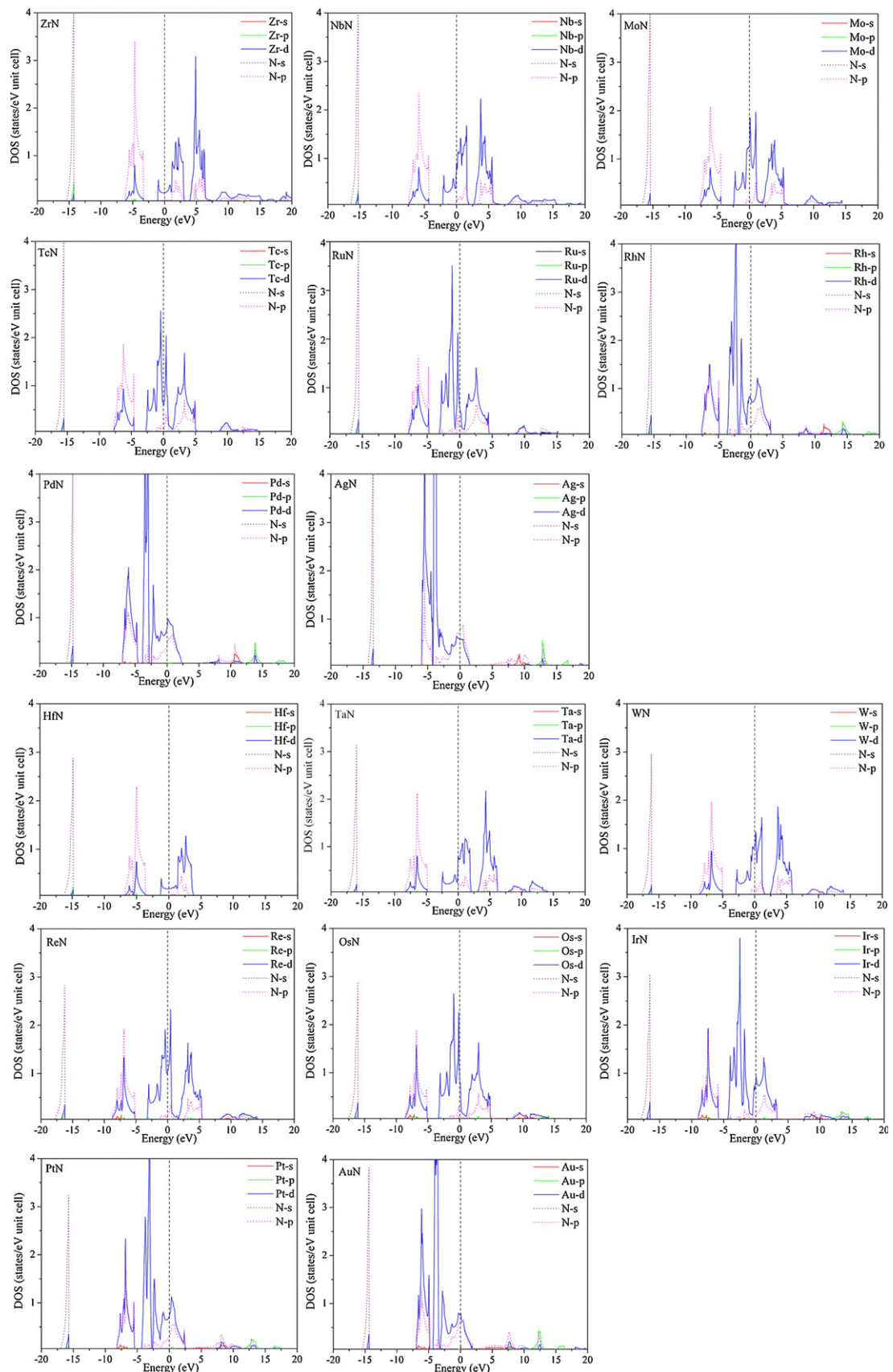


Fig. 4. Partial density of states of transition metal mononitrides for zinc-blende structure.

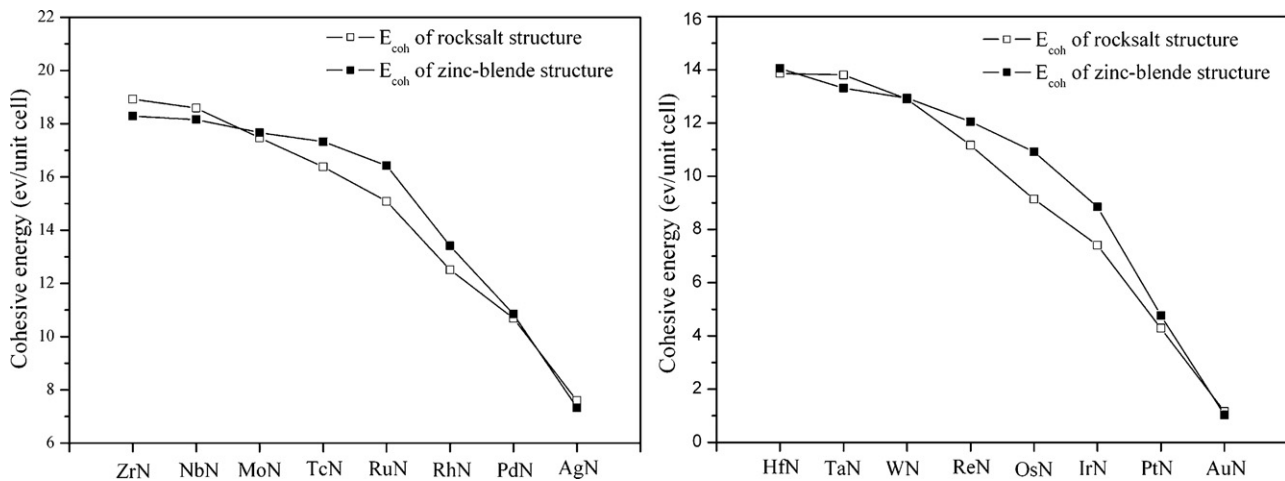


Fig. 5. The cohesive energies of transition metal mononitrides for both rocksalt and zinc-blende structures. Filled squares present the cohesive energies of rocksalt structure and open squares present the cohesive energies of zinc-blende structure.

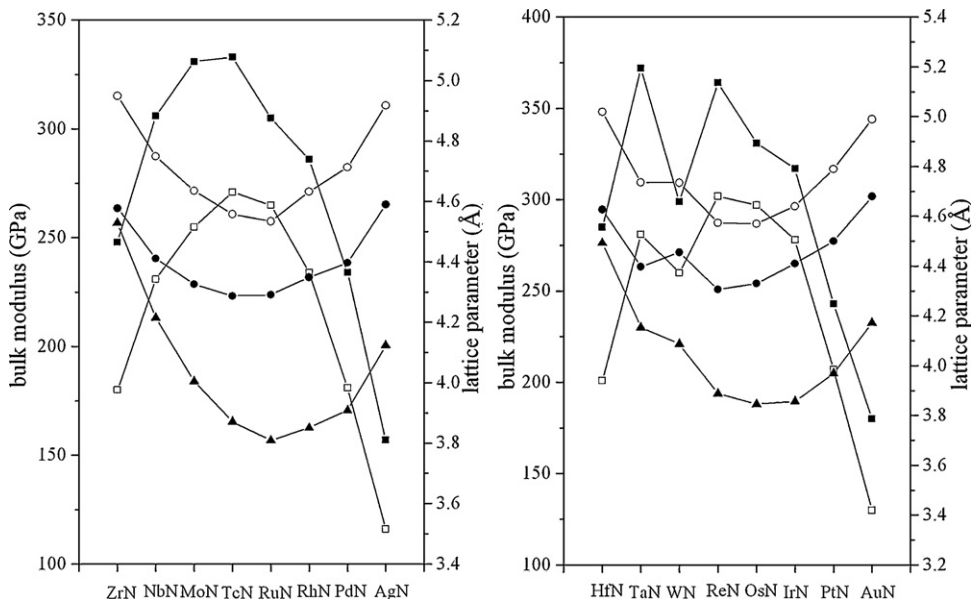


Fig. 6. The bulk moduli of transition metal mononitrides in both rocksalt and zinc-blende structures and equilibrium lattice constants of pure transition metals in the fcc phase and transition metal mononitrides in both rocksalt and zinc-blende structures. Filled and open squares present the bulk moduli of rocksalt structure and zinc-blende structure, respectively. Filled and open circles present the lattice constants of rocksalt structure and zinc-blende structures, respectively. Filled triangles present the equilibrium lattice constants of pure transition metals.

To investigate the correlation between cohesive energies and number of valence electrons, the E_{coh} values of all mononitrides are displayed in Fig. 5. The cohesive energy of MN is calculated as the difference between the total energy of MN compound and its isolated constituent atoms as: $E_{coh}(MN) = (E_M \text{atom} + E_N \text{atom}) - E_{MN} \text{solid}$, where M represents transition metal. For both rocksalt and zinc-blende structures, the largest E_{coh} values are obtained from ZrN and HfN in 4d and 5d series, respectively. From ZrN to AgN in 4d series and HfN to AuN in 5d series, the Fermi level moves farther away from the deep minimum in the density of states (Figs. 3 and 4) and E_{coh} decreases as the number of d electrons increases. It seems that it is more difficult to be synthesized in rocksalt or zinc-blende structures when the compounds have the lower cohesive energy.

In Fig. 6 we display the bulk moduli (B) of transition metal mononitrides in both rocksalt and zinc-blende structures and equilibrium lattice constants of pure transition metals and transition metal mononitrides in both rocksalt and zinc-blende structures. Our results obtained here for pure elements are in good agree-

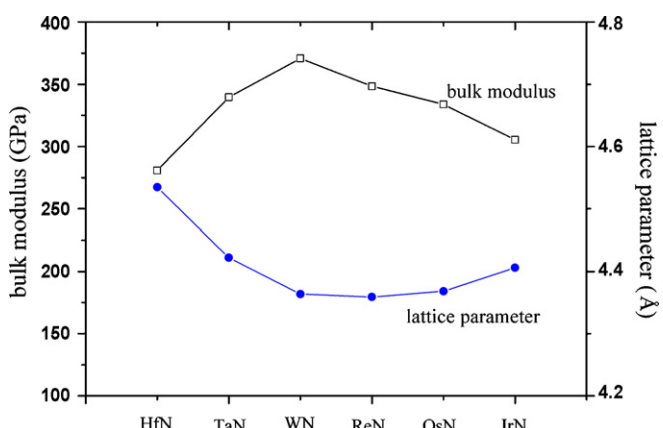


Fig. 7. Trends of lattice parameters (Å) and bulk moduli (GPa) of rocksalt structure calculated by VASP.

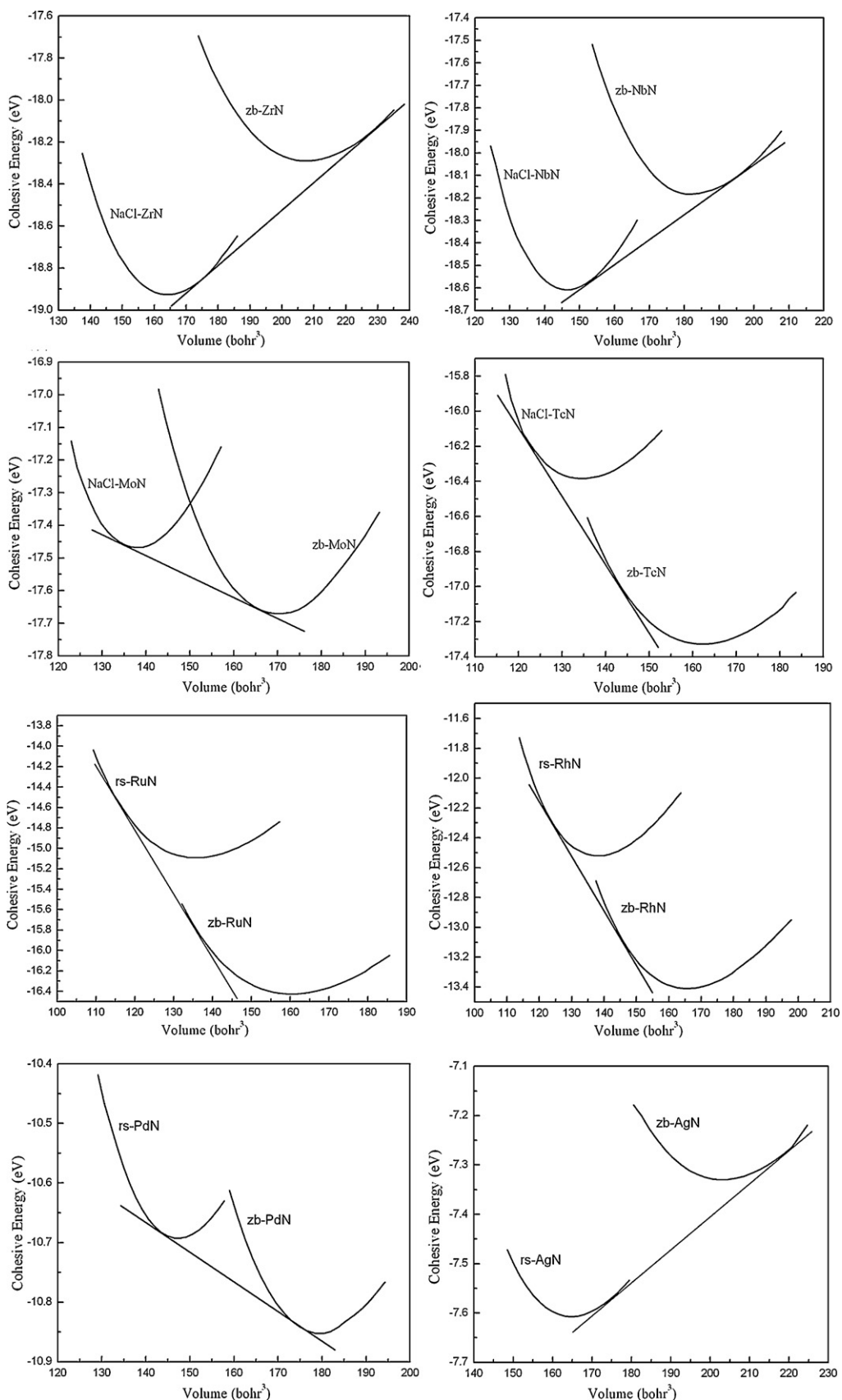


Fig. 8. Cohesive energies as a function of unit-cell volumes for 4d-transition metal mononitrides with both rocksalt and zinc-blende structures.

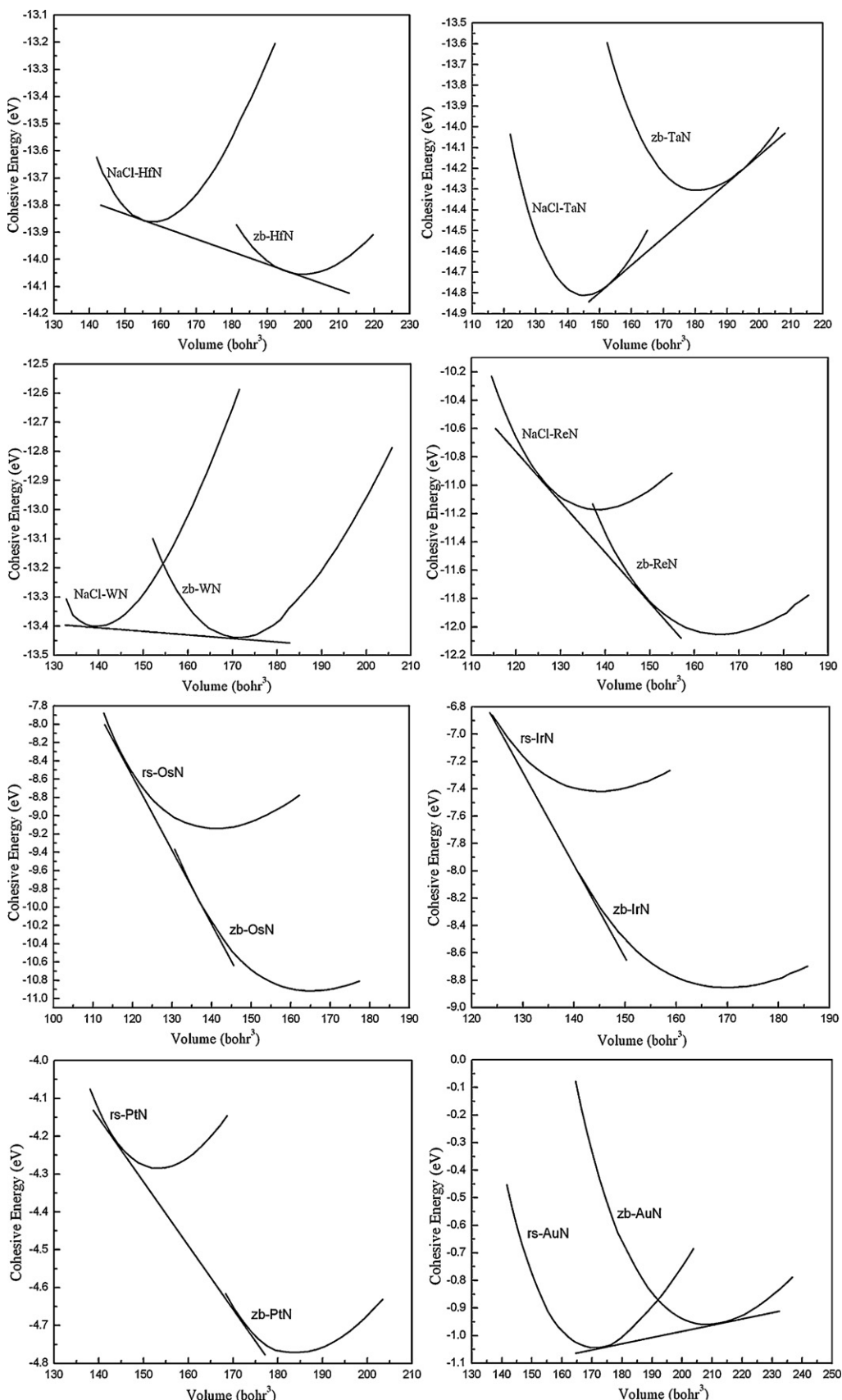


Fig. 9. Cohesive energies as a function of unit-cell volumes for 5d-transition metal mononitrides with both rocksalt and zinc-blende structures.

Table 3

Lattice parameter (\AA) and bulk modulus (GPa) of rocksalt structure calculated by CASTEP and VASP.

	Program	HfN	TaN	WN	ReN	OsN	IrN
Bulk modulus (GPa)	CASTEP	285	372	299	364	331	317
	VASP	281	340	371	348	334	305
Lattice parameter (\AA)	CASTEP	4.56	4.40	4.46	4.31	4.33	4.41
	VASP	4.53	4.42	4.36	4.36	4.37	4.41

Table 4

Transition pressures of zinc-blende-to-rocksalt phase transformations.

	ZrN	NbN	MoN	TcN	RuN	RhN	PdN	AgN
P_{tr} (GPa)	−16	−12	6	45	62	51	5	−7
	HfN	TaN	WN	ReN	OsN	IrN	PtN	AuN
P_{tr} (GPa)	5	−14	2	39	89	72	11	−2

ment with experimental values. The trends of lattice constants for nitrides with rocksalt and zinc-blende structures are consistent with the trends of lattice constants of pure metals with fcc structure as the number of d electrons increases. The lattice constants of rocksalt and zinc-blende structures are larger than those of pure transition metals. Both the rocksalt and zinc-blende structures could be built by introducing N atoms to the octahedral or tetrahedral interstitial sites of the transition metal fcc structure. The lattice constants of zinc-blende type are larger than those of rocksalt type, which should be linked with the fact that the N atoms are located at the tetrahedral site in the fcc structure of the transition metal atoms in zinc-blende structure. This site is rather closer to the neighboring transition metal atoms as compared to the octahedral site of the N atoms in the rocksalt structure. In 4d series, as the number of d electrons of transition metal atoms increases, lattice constant decreases and reaches a minimum at TcN for rocksalt structures, RuN for zinc-blende structures and Ru for pure elements. In 5d series, similar behaviors are detected. The minimums at ReN for both rocksalt and zinc-blende structures and Os for pure elements are found. Bulk modulus, B , does have an opposite behavior for both rocksalt and zinc-blende structures in 4d and 5d series. The variations of lattice constant and B with the number of d electrons indicate the occupation of the bonding and anti-bonding states in the metals and nitrides. As a valence shell (the d shell in this case) starts to be filled, the equilibrium lattice constant decreases and B increases because bonding states are being filled whereas lattice constant increases and B decreases as the anti-bonding states start to be filled. This leads to a minimum of the lattice constants and a maximum of the bulk moduli for the compounds near the half-filled shell. However, WN with rocksalt and zinc-blende structures and pure element W exhibit somewhat anomalous in lattice parameters and bulk moduli. We recalculated the lattice parameters and bulk moduli of mononitrides from HfN to IrN in rocksalt structure using VASP program and all results are listed in Table 3. It is found that except WN, for the other compounds, the results calculated by CASTEP fit well with the results calculated by VASP. The trends of lattice parameters and bulk moduli of WN calculated by VASP also fit well with former analysis results (see in Fig. 7). This indicates that there is some problem with the pseudopotential of W in CASTEP program used here and the pseudopotentials of the other elements are right [46].

Figs. 8 and 9 plot cohesive energies as a function of unit-cell volumes for rocksalt and zinc-blende typed nitrides for 4d- and 5d-transition metal mononitrides, respectively. It is found that except ZrN, NbN, AgN, TaN and AuN, zinc-blende typed nitrides are more energetically stable than rocksalt typed nitrides, which can also be seen from the transition pressures of zinc-blende-to-rocksalt phase transformations, estimated from the slopes of tangent lines

in Table 4. For 4d-transition metal nitrides, the transition pressure increases as the number of d electrons increases, reaches the maximum for RuN, and then decreases to the end of the series. Except HfN, the 5d series have the same trends, reaching the maximum value for OsN. These results are further supported by the difference of E_{coh} between rocksalt structure and zinc-blende structure in Fig. 5, which reaches the maximum in the middle of the series.

4. Conclusions

The electronic and elastic properties of 4d- and 5d-transition metal mononitrides have been studied by first-principles calculations. The calculated results fit well with the available experimental data. It is found that the latest synthesized noble metal nitrides can have neither rocksalt structure nor zinc-blende structure. All metal mononitrides studied in our work are metallic, rather than semiconductor. As the number of d electrons increases, the Fermi level moves farther away from the deep minimum in the density of states and E_{coh} decreases. As the valence shell (the d shell in this case) starts to be filled, the equilibrium lattice constant decreases and bulk modulus increases because bonding states are being filled while lattice constant increases and bulk modulus decreases as the anti-bonding states are filled. This leads to a minimum of the lattice constants and a maximum of the bulk moduli for the compounds near the half-filled shell. The present systematic investigation of 4d- and 5d-transition metal mononitrides may help to identify structural and electronic properties of metal nitrides, which may help to synthesize the potential mononitrides with rocksalt or zinc-blende structures.

Acknowledgements

The calculations were performed at the Shanghai Supercomputer Center. Financial supports from the National Natural Science Foundation of China (Grant Nos. 60776014, 60876002, 10804096, 50920105101, and 10979002), Zhejiang University-Helmholtz Cooperation Fund, the Ministry of Education of China (Program for Changjiang Scholars and the Research Fund for the Doctoral Program of Higher Education), the Department of Science and Technology of Zhejiang province and the Baoyugang Foundation of Zhejiang University are gratefully acknowledged.

References

- [1] S.-H. Jhi, J. Ihm, S.G. Louie, M.I. Cohen, Nature (London) 399 (1999) 132.
- [2] P.F. McMillan, Nat. Mater. 1 (2002) 19.
- [3] T. Maruyama, T. Morishita, Appl. Phys. Lett. 69 (1996) 890.
- [4] S. Yamanaka, K. Hotehama, H. Kawaji, Nature (London) 392 (1998) 580.
- [5] A. Zerr, G. Miehe, R. Boehler, Nat. Mater. 2 (2003) 185.

- [6] M. Chhowalla, H.E. Unalan, *Nat. Mater.* 4 (2005) 317.
- [7] A. Leineweber, H. Jacobs, S. Hull, *Inorg. Chem.* 40 (2001) 5818.
- [8] Z.G. Wu, X.J. Chen, V.V. Struzhkin, R.E. Cohen, *Phys. Rev. B* 71 (2005) 214103.
- [9] E. Gregoryanz, C. Sanloup, M. Somayazulu, J. Badro, G. Fiquet, H.-K. Mao, R. Hemeley, *Nat. Mater.* 3 (2004) 294.
- [10] J.C. Crowhurst, A.F. Goncharov, B. Sadigh, C.L. Evans, P.G. Morrall, J.L. Ferreira, A.J. Nelson, *Science* 311 (2006) 1275.
- [11] A.F. Young, C. Sanloup, E. Gregoryanz, S. Scandolo, R.J. Hemley, H.K. Mao, *Phys. Rev. Lett.* 96 (2006) 155501.
- [12] J.C. Crowhurst, A.F. Goncharov, B. Sadigh, J.M. Zaug, D. Aberg, Y. Meng, V.B. Prakapenka, *J. Mater. Res.* 23 (2008) 1–5.
- [13] B.R. Sahu, L. Kleinman, *Phys. Rev. B* 71 (2005) 041101.
- [14] J. Uddin, G.E. Scuseria, *Phys. Rev. B* 72 (2005) 035101.
- [15] M.B. Kanoun, S. Goumri-Said, *Phys. Rev. B* 72 (2005) 113103.
- [16] R. Yu, X.F. Zhang, *Appl. Phys. Lett.* 86 (2005) 121913.
- [17] R. Yu, X.F. Zhang, *Phys. Rev. B* 72 (2005) 054103.
- [18] R. Yu, Q. Zhan, X.F. Zhang, *Appl. Phys. Lett.* 88 (2006) 051913.
- [19] S.K.R. Patil, S.V. Khare, B.R. Tuttle, J.K. Bording, S. Kodambaka, *Phys. Rev. B* 73 (2006) 104118.
- [20] A.F. Young, J.A. Montoya, C. Sanloup, M. Lazzeri, E. Gregoryanz, S. Scandolo, *Phys. Rev. B* 73 (2006) 153102.
- [21] C.Z. Fan, S.Y. Zeng, L.X. Li, Z.J. Zhan, R.P. Liu, W.K. Wang, P. Zhang, Y.G. Yao, *Phys. Rev. B* 74 (2006) 125118.
- [22] R. Yu, Q. Zhan, C. De Jonghe, *Angew. Chem., Int. Ed.* 46 (2007) 1136.
- [23] J.A. Montoya, A.D. Hernandez, C. Sanloup, E. Gregoryanz, S. Scandolo, *Appl. Phys. Lett.* 90 (2007) 011909.
- [24] D. Aberg, B. Sadigh, J. Crowhurst, F. Goncharov, *Phys. Rev. Lett.* 100 (2008) 095501.
- [25] N. Bettahar, S. Benalia, D. Rached, M. Ameri, R. Khenata, H. Baltache, H. Rached, *J. Alloys Compd.* 478 (2009) 297–302.
- [26] J. Zhou, Z.M. Sun, R. Ahuja, *J. Alloys Compd.* 472 (2009) 425–428.
- [27] X.W. Zhang, G. Trinarchi, A. Zunger, *Phys. Rev. B* 79 (2009) 092102.
- [28] W. Chen, J.S. Tse, J.Z. Jiang, *J. Phys.: Condens. Matter* 22 (2010) 015404.
- [29] W. Chen, J.S. Tse, J.Z. Jiang, *Solid State Commun.* 150 (2010) 181.
- [30] K. Suzuki, T. Kaneko, H. Yoshida, H. Morita, H. Fujimori, *J. Alloys Compd.* 224 (1995) 232.
- [31] R. De Paiva, R.A. Nogueira, J.L.A. Alves, *Braz. J. Phys.* 36 (2006) 470.
- [32] R. De Paiva, R.A. Nogueira, J.L.A. Alves, *Phys. Rev. B* 75 (2007) 085105.
- [33] W.J. Zhao, Z.J. Wu, *J. Solid State Chem.* 181 (2008) 2814–2827.
- [34] B. Hong, L. Cheng, M.Y. Wang, Z.J. Wu, *Mol. Phys.* 108 (2010) 25–33.
- [35] Materials studio, Version 3.2, Accelrys Inc., 2002.
- [36] D. Vanderbilt, *Phys. Rev. B* 41 (1990) 7892.
- [37] D.M. Ceperley, B.J. Alder, *Phys. Rev. Lett.* 45 (1980) 566.
- [38] J.P. Perdew, Y. Wang, *Phys. Rev. B* 45 (1992) 13244.
- [39] F.D. Murnaghan, *Proc. Natl. Acad. Sci. U.S.A.* 30 (1944) 244.
- [40] S.Q. Wu, Z.F. Hou, Z.Z. Zhu, *Solid State Commun.* 143 (2007) 425.
- [41] J. Haines, J.M. Leger, G. Bocquillon, *Annu. Rev. Mater. Res.* 31 (2001) 1.
- [42] W.B. Pearson (Ed.), *Structure Reports (International Union of Crystallography)*, Oosthoek, Scheltema, and Holkema, Utrecht, 1913–1993.
- [43] X.-J. Chen, V.V. Struzhkin, Z. Wu, M. Somayazulu, J. Qian, S. Kung, A.N. Christens, Y. Zhao, R.E. Cohen, H.-K. Mao, R.J. Hemley, *Proc. Natl. Acad. Sci. U.S.A.* 102 (2005) 3198.
- [44] J.F. Nye, *Physical Properties of Crystals*, Oxford University Press, Oxford, 1985.
- [45] W.A. Harrison, G.K. Straub, *Phys. Rev. B* 36 (1987) 2695.
- [46] We contacted with CASTEP dealer and they confirmed that the CASTEP version 3.2 indeed has a bad pseudopotential for W and good pseudopotentials for the other elements studied here.